Optical absorbence and band structure of molecular hydrogen in different phases

Original Research Article

Abstract

In this article optical absorbing and band structure of solid molecular hydrogen at five different phases are reported. Transition pressure from non-metallic phase to metallic phase is found at 284 GPA. Phase-IV and phase-V of solid molecular hydrogen are assumed to be metallic. It is also observed that UV-visible spectra of molecular hydrogen is also changing significantly with the change of pressure.

Keywords: ***Hydrogen molecular solid; Electrical conductivity; Transition pressure; Configuration Interaction; Critical density; band structure***

PACS : 31.70.ks, 31.90

1 Introduction

Determining the metalization pressure of solid hydrogen is of great interest due to the the possible existence of room-temperature superconductivity [1] and a metallic liquid ground state [2]. There are both dynamic [3] and static experiments [4, 5, 6, 7] and theoretical calculations [8, 9, 10, 11, 12, 13]. So far five different phases of solid hydrogen are proposed. Phase I is a molecular solid composed of quantum rotors arranged in a hexagonal close-packed structure. It is stable up to 110 GPa. Phase II is known as broken-symmetry phase. It exists within 110 GPa to 150 GPa pressure range. Phases I and II have different parity of the rotational states namely ortho-para distinction [14]. In contrast, phase III

---

is accompanied by a large discontinuity in the Raman spectrum. The strong rise in its spectral weight of molecular vibrons is due to orientationally ordered structure. Phase IV is reported above 230 GPa pressure at 300K. The most recent experimental results [15] suggests that there may exists another phase of hydrogen above 325 GPa pressure and 300K temperature. This proposed phase V, may meet phases I and IV at a triple point where hydrogen retains its molecular character.

It is observed that with increase of pressure, fundamental vibrational frequency and the low-frequency excitations are partially lost [16]. Thus, Density Functional Theory (DFT) calculations are performed to study the change of optical absorbence and vibrational frequency shift of molecular hydrogen with the increase of pressure. Band structures are computed taking different pressure for five different solid phases of molecular hydrogen.

2 Theoretical Background for DC conductivity calculation using conversion parameter

DC conductivity (σ) of an electrical conductor is the ratio of the current density ($\hat{J}$) and the applied electrical potential (E). Current density ($\hat{J}$) for DC potential is given as

$$\hat{J} = -nev \tag{2.1}$$

where, n is the number of electrons per cubic centimeter, e is the charge of electron and v is the average velocity of electron due to the applied electric field. For unit potential, $\hat{J} = \sigma$. Thus, we can write

$$\sigma = -nev \tag{2.2}$$

Here ne is the electronic charge density in the valance band. Thus, ne is proportional to the electron's probability density in the valance band. Considering electron pair hopping we can say, when electrical field is applied, electron transfer occurs from one molecular site to another. Quantum technique may be used to verify whether electron transfer from one site to another site of a system is possible or not. For electrical conductors electron transfer must be quantum mechanically allowed and transfer integral would be positive in sign as DC conductivity is proportional to the square root of the transfer integral [8]. If we replace electronic velocity (v) by $\sqrt{KE}$ in Equation 2.2, where KE is the kinetic energy integral of electrons in the valance orbital we shall get an expression for the calculation of electrical conductivity. Thus, DC conductivity may be defined in terms of charge density and kinetic energy as

$$\sigma = B_a \rho e \sqrt{KE} \tag{2.3}$$

where ρe is charge density of valance electron and B_a is the proportionality constant known as conversion parameter [8]. If we know the value of valence electron density and transfer integral of any conductor we shall get the value of electrical conductivity of that conductor at any temperature provided that value of B_a at that temperature is known. From Equation 2.3 it is obvious that a positive value of KE implies electron transfer is quantum mechanically allowed. On the other hand, 0 or negative value of KE implies that the respective process is forbidden.

3 Computational Details

Configuration Interaction (CI) [17, 18] theory is used for the calculation of charge density of the conductor. Transfer integrals (kinetic energy integral, KE in particular) are calculated for different CI populations. In this process only pair hopping is considered. GAMESS (Version = 6 SEP 2001 (R5) from Iowa State University) [19] is used for Hartree Fock level calculation. STO-3G basis set is used for all calculations. ρe is calculated from overlap matrix and density matrix. KE is calculated from overlap between different CI states. Conductivity is calculated from Equation 2.3.

Density functional based calculations are done using GAUSSIAN 09 [20]. Optical absorbence is computed using time dependent density functional theory (TDDFT) [21]. Beckes three parameter of hybrid exchange functional [22] combined with Lee$-$Yang$-$Parr non-local correlation function [23], abbreviated as B3LYP is used for all DFT calculations. This functional is used because it is proved that for spectral properties this functional reproduce experimental results very accurately [24, 25, 26, 27, 28, 29, 30, 31, 32].

Conversion parameter (B_a) at different temperatures are calculated from the plot of B_a vs $T(K)$. For this plot, B_a values of Li and Mg at different temperatures are taken from Reference [8]. B_a vs $T(K)$ is plotted for Li, Mg and $average$ of these two (Figure 1). QUANTUM ESPRESSO [33], a modular and open-source software project for quantum simulations of materials is used for solid state calculations.

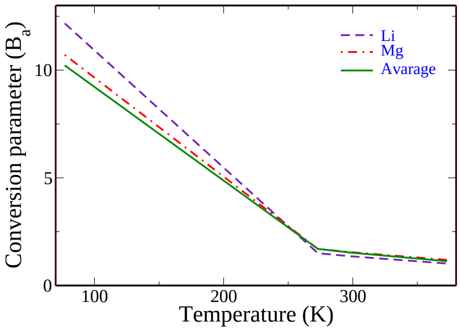

Figure 1: Variation of conversion parameter with respect to temperature

4 Result and Discussion

4.1 Transition geometry of hydrogen molecular solid from non-metallic phase to metallic phase

Kinetic energy integral for different $H_2 - H_2$ molecular distances are taken from reference [8] and plotted against molecular distance which is presented in Figure 2. It is observed that KE variation with molecular distance is not linear. It varies in a zig zag way. At $H_2 - H_2$

distance of $1.72\AA$ kinetic energy (KE) plot crosses X-axis. Thus, we may conclude that this $H_2 - H_2$ distance is the transition point of molecular hydrogen to metallic hydrogen. It is reported [8] that pressure at the transition state is 2.8 Mbar or 280 GPa. Calculated density of metallic hydrogen is $1.302\ gm\ cm^3$. Experimental results reported by Grigorev et al [35] shows that at transition point density of hydrogen is within 1.08 to $1.30\ gm\ cm^3$. Thus, this $H_2 - H_2$ distance is taken for band structure calculation.

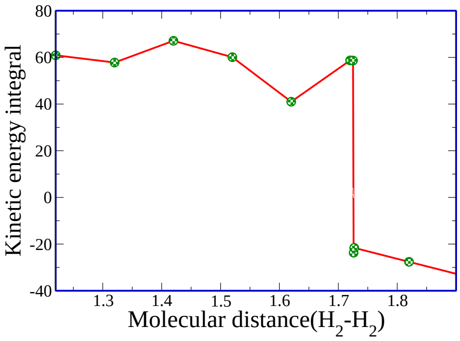

Figure 2: Change of kinetic energy integral with respect to molecular distance

4.2 Change of optical absorptivity due to the change of molecular distance

Using the time dependent density functional theory (TDDFT) calculation, UV-visible spectra of hydrogen molecular solid for different $H_2 - H_2$ distances are computed. $1.6\AA$, $1.7\AA$, $1.8\AA$ and $2.1\AA$ molecular distances are taken for this computation. These values are chosen as we know $1.7\AA$ is the molecular distance at the transition point. $1.6\AA$ and $1.8\AA$ are the molecular distances above and bellow the transition point respectively. $2.1\AA$ molecular distance is taken to know the spectral pattern shortly away from the transition point. Computed spectra are presented in Figure 3.

There are five distinct peak points in the UV-visible spectrum when two H_2 molecules are separated by $2.1\AA$ distance. The peaks are at $91nm$, $78nm$, $56nm$, $46nm$ and $44nm$. Spectral pattern changes with decrease of inter molecular distance. At $1.8\AA$ lowest energy peak $(91nm)$ doesn't shifted. But second $(76nm)$, third $(54nm)$ and fifth $(42nm)$ show blue shift while fourth $(48nm)$ peak shows red shift. The third peak practically vanishes at $1.7\AA$ and $1.6\AA$ molecular distance. Red shift of fourth peak continues $(49nm$ and $50nm$ respectively). Position of second (at $76nm$) and fifth peak (at $42nm$) don't change with further change of molecular distance. But, little red shift is observed for the first peak $(92nm$ and $93nm$ respectively). Intensity ratio of the fourth and fifth peak changes with decrease of molecular distances. At $1.6\AA$ molecular distance intensity of the fourth peak is greater than that of the fifth peak.

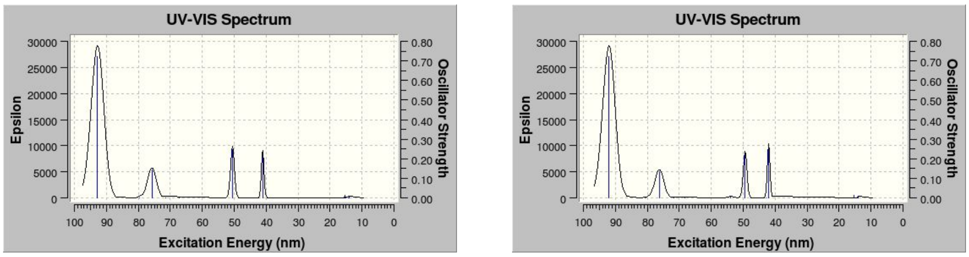

(a) distance = $1.6\mathring{A}$ (b) distance = $1.7\mathring{A}$

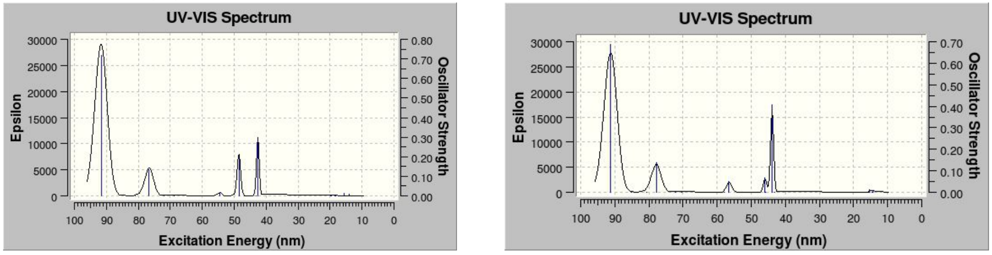

(c) distance = $1.8\mathring{A}$ (d) distance = $2.1\mathring{A}$

Figure 3: Change of optical absorptivity with respect to molecular distance

4.3 Band structures of molecular solid hydrogen in different phases

Computed band structures of solid molecular hydrogen at five different phases are presented in Figure 4. The variation of band gap due to the change of pressure is presented in Table 1.

Table 1: Change of band gap due to the change of pressure

Phase	Pressure (GPa)	Band gap (eV)
Phase-I	90	1.5
Phase-II	138	0.6
Phase-III	211	0.2
Phase-IV	284	0.0
Phase-V	332	0.0

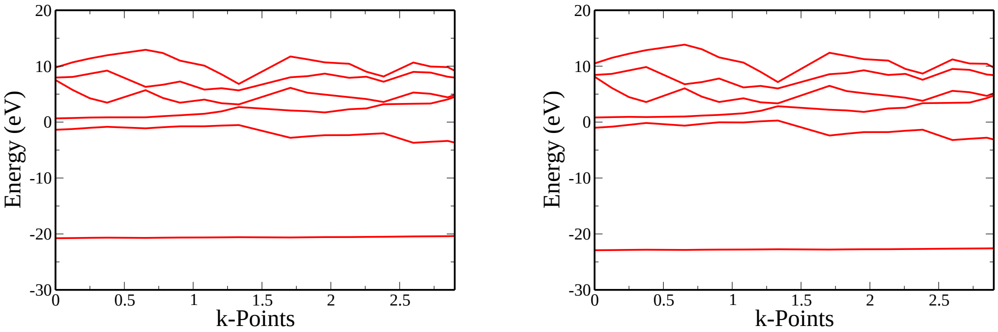

(a) 90 GPa (b) 138 GPa

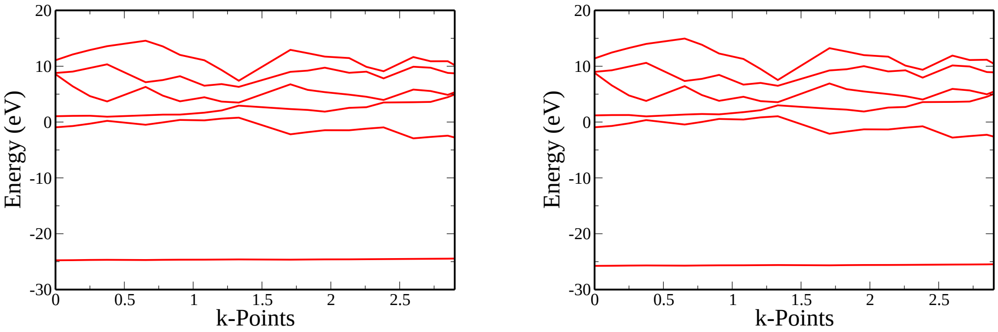

(c) 211 GPa (d) 284 GPa

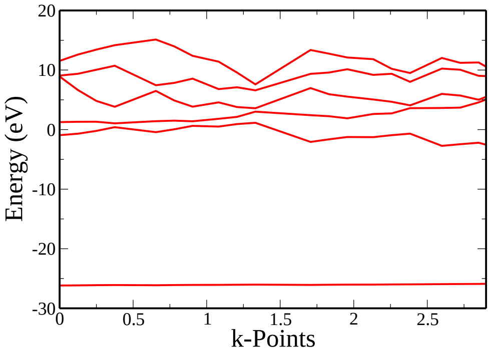

(e) 332 GPa

Figure 4: Change of band structure with respect to pressure

It is observed that band gap decreases with the increase of pressure. From the band gap values we may conclude that phase-IV and phase-V of solid molecular hydrogen are metallic phase. Non metallic to metallic phase transition occurs near at 284 GPa pressure which is similar to the value $(280$ GPa) obtained by transfer integral (kinetic energy integral) calculation method [8]. Phase-II and phase-III are like semiconductor, while phase-I is like non-metallic. It is also observed that though band gap decreases with increase of pressure, nature of the band doesn't change.

5 Conclusions

Band gap and optical spectra of solid molecular hydrogen significantly changes with increase of pressure. It is very difficult to predict the transition pressure of a molecular solid to the metallic phase by studding only the band gap or band structure as the changes are very small when the change of pressure is very small. But, calculation of transition pressure is comparatively easier by by transfer integral (kinetic energy integral) calculation method [8]. Not only that, from the kinetic energy integral value, we can calculate the electrical conductivity of a metal with the help of conversion parameter at different temperatures.

References

[1] Neil W Ashcroft. Metallic hydrogen: a high-temperature superconductor? *Physical Review Letters*, 21(26):1748, 1968.

[2] Stanimir A Bonev, Eric Schwegler, Tadashi Ogitsu, and Giulia Galli. A quantum fluid of metallic hydrogen suggested by first-principles calculations. *Nature*, 431(7009):669–672, 2004.

[3] ST Weir, AC Mitchell, and WJ Nellis. Metallization of fluid molecular hydrogen at 140 gpa (1.4 mbar). *Physical Review Letters*, 76(11):1860, 1996.

[4] Isaac F Silvera and Rinke J Wijngaarden. New low-temperature phase of molecular deuterium at ultrahigh pressure. *Physical Review Letters*, 47(1):39, 1981.

[5] Ho-kwang Mao and Russell J Hemley. Ultrahigh-pressure transitions in solid hydrogen. *Reviews of modern physics*, 66(2):671, 1994.

[6] II Mazin, Russell J Hemley, AF Goncharov, Michael Hanfland, and Ho-kwang Mao. Quantum and classical orientational ordering in solid hydrogen. *Physical review letters*, 78(6):1066, 1997.

[7] Ross T Howie, Christophe L Guillaume, Thomas Scheler, Alexander F Goncharov, and Eugene Gregoryanz. Mixed molecular and atomic phase of dense hydrogen. *Physical Review Letters*, 108(12):125501, 2012.

[8] Arijit Bag. Pressure effect on electrical conductivity of hydrogen molecular solid: Quantum mechanical approach. *Journal of Electrical and Electronics Engineerning*, 2(7):30, 2015.

[9] Hikaru Kitamura, Shinji Tsuneyuki, Tadashi Ogitsu, and Takashi Miyake. Quantum distribution of protons in solid molecular hydrogen at megabar pressures. *Nature*, 404(6775):259–262, 2000.

[10] Kurt A Johnson and NW Ashcroft. Structure and bandgap closure in dense hydrogen. *Nature*, 403(6770):632–635, 2000.

[11] Chris J Pickard and Richard J Needs. Structure of phase iii of solid hydrogen. *Nature Physics*, 3(7):473–476, 2007.

[12] Egor Babaev, Asle Sudbø, and NW Ashcroft. A superconductor to superfluid phase transition in liquid metallic hydrogen. *Nature*, 431(7009):666–668, 2004.

[13] Alexander F Goncharov, S Tse John, Hui Wang, Jianjun Yang, Viktor V Struzhkin, Ross T Howie, and Eugene Gregoryanz. Bonding, structures, and band gap closure of hydrogen at high pressures. *Physical Review B*, 87(2):024101, 2013.

[14] Isaac F Silvera. The solid molecular hydrogens in the condensed phase: Fundamentals and static properties. *Reviews of Modern Physics*, 52(2):393, 1980.

[15] Philip Dalladay-Simpson, Ross T Howie, and Eugene Gregoryanz. Evidence for a new phase of dense hydrogen above 325 gigapascals. *Nature*, 529(7584):63–67, 2016.

[16] Sam Azadi, Neil David Drummond, and WMC Foulkes. Nature of the metallization transition in solid hydrogen. *Physical Review B*, 95(3):035142, 2017.

[17] John A Pople, J Stephen Binkley, and Rolf Seeger. Theoretical models incorporating electron correlation. *International Journal of Quantum Chemistry*, 10(S10):1–19, 1976.

[18] SF Boys. Electronic wave functions. ii. a calculation for the ground state of the beryllium atom. In *Proceedings of the Royal Society of London A: Mathematical, Physical and Engineering Sciences*, volume 201, pages 125–137. The Royal Society, 1950.

[19] Michael W Schmidt, Kim K Baldridge, Jerry A Boatz, Steven T Elbert, Mark S Gordon, Jan H Jensen, Shiro Koseki, Nikita Matsunaga, Kiet A Nguyen, Shujun Su, et al. General atomic and molecular electronic structure system. *Journal of computational chemistry*, 14(11):1347–1363, 1993.

[20] M. J. Frisch, G. W. Trucks, H. B. Schlegel, G. E. Scuseria, M. A. Robb, J. R. Cheeseman, G. Scalmani, V. Barone, B. Mennucci, G. A. Petersson, H. Nakatsuji, M. Caricato, X. Li, H. P. Hratchian, A. F. Izmaylov, J. Bloino, G. Zheng, J. L. Sonnenberg, M. Hada, M. Ehara, K. Toyota, R. Fukuda, J. Hasegawa, M. Ishida, T. Nakajima, Y. Honda, O. Kitao, H. Nakai, T. Vreven, J. A. Montgomery, J. E. Peralta Jr., F. Ogliaro, M. Bearpark, J. J. Heyd, E. Brothers, K. N. Kudin, V. N. Staroverov, R. Kobayashi, J. Normand, K. Raghavachari, A. Rendell, J. C. Burant, S. S. Iyengar, J. Tomasi, M. Cossi, N. Rega, J. M. Millam, M. Klene, J. E. Knox, J. B. Cross, V. Bakken, C. Adamo, J. Jaramillo, R. Gomperts, R. E. Stratmann, O. Yazyev, A. J. Austin, R. Cammi, C. Pomelli, J. W. Ochterski, R. L. Martin, K. Morokuma, V. G. Zakrzewski, G. A. Voth, P. Salvador, J. J. Dannenberg, S. Dapprich, A. D. Daniels, O. Farkas, J. B. Foresman, J. V. Ortiz, J. Cioslowski, and D. J. Fox. *Gaussian 09, Revision D.01*. Gaussian, Inc., Wallingford CT, 2009.

[21] E. Runge and E. K. U. Gross. Density functional theory for time dependent systems. *Phys. Rev. Lett.*, 52(12):997–1000, 1984.

[22] A. D. Becke. *Phys. Rev. A*, 38:3098–3100, 1988.

[23] C. Lee, W. Yang, and R. G. Parr. *Phys. Rev. B*, 37:785–789, 1988.

[24] Arijit Bag and Pradip Kr. Ghorai. Computational investigation of the ligand field effect to improve photoacoustic properties of organometallic carbonyl clusters. *RSC Adv.*, 5(40):31575–31583, 2015.

[25] Arijit Bag and Pradip Kr Ghorai. Enhancement of biocompatibility and photoacoustic contrast activity of metal clusters. *Journal of Molecular Graphics and Modelling*, 2017.

[26] Arijit Bag. Application of glucose modified bicyclophosphite derivative of tri-ruthenium carbonyl cluster as advanced photo acoustic contrast agent. *Saudi J. Med. Pharm. Sci*, 1(3):80–82, 2015.

[27] S. Chiodo, N. Russo, and E. Sicilia. *J. Chem. Phys.*, 125:104107 – 104107–8, 2006.

[28] J. F. Alvino, T. Bennett, D. Anderson, B. Donoeva, D. Ovoshchnikov, R. H. Adnan, D. Appadoo, V. Golovko, G. Andersson, and G. F. Metha. *RSC Adv.*, 3:22140–22149, 2013.

[29] T. Bennett, R. H. Adnan, J. F. Alvino, V. Golovko, G. G. Andersson, and G. F. Metha. *Inorg. Chem.*, 53:4340–4349, 2014.

[30] H. Wang, Y. Xie, R. B. King, and III H. F. Schaefer. *J. Am. Chem. Soc.*, 128:11376–11384, 2006.

[31] T. Andruniow, M. Jaworska, P. Lodowski, M. Z. Zgierski, R. Dreos, L. Randaccio, and P. M. Kozlowski. *J. Chem. Phys.*, 129:085101 – 085101–14, 2008.

[32] M. R. Silva-Junior, M. Schreiber, S. P. A. Sauer, and W. Thiel. *J. Chem. Phys.*, 129:104103 – 104103–14, 2008.

[33] Paolo Giannozzi, Stefano Baroni, Nicola Bonini, Matteo Calandra, Roberto Car, Carlo Cavazzoni, Davide Ceresoli, Guido L Chiarotti, Matteo Cococcioni, Ismaila Dabo, Andrea Dal Corso, Stefano de Gironcoli, Stefano Fabris, Guido Fratesi, Ralph Gebauer, Uwe Gerstmann, Christos Gougoussis, Anton Kokalj, Michele Lazzeri, Layla Martin-Samos, Nicola Marzari, Francesco Mauri, Riccardo Mazzarello, Stefano Paolini, Alfredo Pasquarello, Lorenzo Paulatto, Carlo Sbraccia, Sandro Scandolo, Gabriele Sclauzero, Ari P Seitsonen, Alexander Smogunov, Paolo Umari, and Renata M Wentzcovitch. Quantum espresso: a modular and open-source software project for quantum simulations of materials. *Journal of Physics: Condensed Matter*, 21(39):395502, 2009.

[34] David E Ramaker, Lalit Kumar, and Frank E Harris. Exact-exchange crystal hartree-fock calculations of molecular and metallic hydrogen and their transitions. *Physical Review Letters*, 34(13):812, 1975.

[35] FV Grigor'ev, SB Kormer, OL Mikhailova, AP Tolochko, and VD Urlin. Experimental determination of the compressibility of hydrogen at densities 0.5-2 g/cm3. metallization of hydrogen. *ZhETF Pisma Redaktsiiu*, 16:286, 1972.